PPPL-2224 PPPL-2224

UC20-A,F

DE 1175.4

CONF-850310--116

I-22143

CONFINEMENT STUDIES IN TFTR

By

M. Murakami et al.

JUNE 1985

PLASMA PHYSICS LABORATORY

PRINCETON UNIVERSITY
PRINCETON, NEW JERSEY

PREPARED FOR THE U.S. DEPARTMENT OF ENERGY,
UNDER CONTRACT DE-AC02-76-CHO-3073.

CONFINEMENT STUDIES IN TFTR*

M. Murakami[a], V. Arunasalam, J.D. Bell[a], M.G. Bell, M. Bitter, W.R. Blanchard, F. Boody, D. Boyd[b], N. Bretz, C.E. Bush[a], J.D. Callen[c], J.L. Cecchi, R.J. Colchin[a], J. Coonrod, S.L. Davis, D. Dimock, H.F. Dyll. P.C. Efthimion, L.C. Emerson[a], A.C. England[a], H.P. Eubank, R. Fonck, E. Fredrickson, H.P. Furth, L.R. Grisham, S. von Goeler, R.J. Goldston, B. Grek, D.J. Grove, R.J. Hawryluk, H. Hendel[d], K.W. Hill, R. Hulse, D. Johnson, L.C. Johnson, R. Kaita, J. Kamperschroer, S.M. Kaye, M. Kikuchi[e], S. Kilpatrick, H. Kugel, P.H. LaMarche, R. Little, C.H. Ma[a], D. Manos, D. Mansfield, M. McCarthy, R.T. McCann, D.C. McCune, K. McGuire, D.M. Meade, S.S. Medley, D.R. Mikkelsen, D. Mueller, E. Nieschmidt[f], D.K. Owens, V.K. Pare[a], H. Park, B. Prichard, A. Ramsey, D.A. Rasmussen[a], A.L. Roquemore, P.H. Rutherford, N.R. Sauthoff, J. Schivell, J-L. Schwob[g], S.D. Scott, S. Sesnic, M. Shimada[e], J.E. Simpkins[a], J. Sinnis, F. Stauffer[b], B. Stratton, S. Suckewer, G.D. Tait, G. Taylor, F. Tenney, C.E. Thomas[a], H.H. Towner, M. Ulrickson, R. Wieland, M. Williams, K-L. Wong, A. Wouters, H. Yamada[h], S. Yoshikawa, K.M. Young, and M.C. Zarnstorff

Plasma Physics Laboratory, Princeton University
P.O. Box 451, Princeton, NJ 08544

[a]Permanent address: Oak Ridge National Laboratory, Oak Ridge, TN
[b]Permanent address: University of Maryland, College Park, MD
[c]Permanent address: University of Wisconsin, Madison, WI
[d]Permanent address: RCA David Sarnoff Research Center, Princeton, NJ
[e]Permanent address: Japan Atomic Energy Research Institute, Japan
[f]Permanent address: EG&G, Idaho
[g]Permanent address: Hebrew University of Jerusalem, Israel
[h]Permanent address: University of Tokyo, Japan

PPPL--2224

DE85 015305

ABSTRACT

The paper describes the present (end of February 1985) status of the plasma confinement studies in the TFTR tokamak with emphasis on those with neutral beam injection (NBI). Recent improvements in the device capabilities have substantially extended operating parameters: B_T increased to 4.0 T, I_p to 2.0 MA, injection power (P_b) to 5 MW with H° or D° beams, $\bar{n}_e$ to 5×10^{19} m^{-3}, and Z_{eff} reduced to 1.4. With ohmic heating (OH) alone, the previously established scaling for gross energy confinement time ($\tau_E \propto \bar{n}_e q$) has been confirmed at higher I_p and B_T, and the maximum τ_E of 0.4 sec has been achieved. With NBI at P_b substantially (by factor > 2) higher than P_{OH}, excellent power and particle accountability have been established. This suggests that the less-than-expected increase in stored energy with NBI is not due to problems of power delivery, but due to problems of confinement deterioration. τ_E is observed to scale approximately as $I_p P_b^{-0.5}$ (independent of $\bar{n}_e$), consistent with previous L-mode scalings. With NBI we have achieved the maximum τ_E of 0.2 sec and the maximum $T_i(o)$ of 4.4 keV in the normal operating regime, and even higher $T_i(o)$ in the energetic-ion regime with low-n_e and low-I_p operation.

I. INTRODUCTION

The research goals of the Tokamak Fusion Test Reactor (TFTR) are to study plasma confinement at fusion reactor plasma parameters and to demonstrate energy breakeven with DT plasmas. For these purposes, a 120 keV, 25-30 MW neutral beam injection (NBI) system will be provided, backed up by adiabatic compression to multiply the effective heating power. Of critical importance in pursuing these goals are transport and stability properties of discharges with auxiliary heating. After the first year of operation with ohmic heating alone,[1-5] the first two of four neutral beamlines, each with three ion sources, were installed on TFTR in the co-tangential direction. Initial neutral beam injection experiments with H° neutral power (P_b) up to 1.2 MW from one beamline started in August 1984, and results were reported at the London IAEA Conference.[6] Since then, the second beamline has been brought into operation with total neutral (H° or D°) power of up to 5 MW.[7] In addition, the TFTR operational capabilities have been upgraded[8]: the toroidal field (B_T) from 2.3 T to 4.0 T; the plasma current (I_p) from 1.4 MA to 2.0 MA; and the effective ion charge (Z_{eff}) down to 1.4. The device capabilities are expected to be

*Presented at the 6th Topical Meeting on the Technology of Fusion Energy, San Francisco, March 1985. The proceedings are to be published in Fusion Technology, July 1985.

further upgraded before shutdown in mid April, 1985. This paper reviews the present (end of February, 1985) status of the confinement studies in TFTR. It emphasizes confinement studies with beam-heated full-size discharges under normal operating conditions. The energetic-ion regime recently attained with high power injection into low-density ($\bar{n}_e$ = 1 x 10^{19} m^{-3}), low-current (I_p = 0.8 MA) discharges is discussed in H. Furth's invited paper.[9]

II. CONFINEMENT OF OHMICALLY HEATED DISCHARGES

There has been substantial improvement in the cleanliness of plasmas in TFTR during this operational period. Daily high current operation ($I_p \geq 1.8$ MA) for many weeks without a vacuum vessel opening coupled with plasma optimization techniques[10] has reduced Z_{eff} below 2.0, as determined by measurements of both the visible bremsstrahlung, neoclassical resistivity, and X-ray pulse height-analysis. In addition, the radiation fraction P_{rad}/P_{OH} has fallen to ~ 40%. The main impurity species in the TFTR plasma is carbon, but there is a substantial contribution to Z_{eff} from nickel and titanium at low densities ($\bar{n}_e$ ~ 1 x 10^{19} m^{-3}) and from oxygen near the high density limit.[11] Near the density limit, MARFE-like phenomena[12] have been observed, and further small increments in plasma density have resulted in major disruptions.[13] Application of chromium gettering[14] has been effective in reducing the oxygen content by a factor of 2.5 without a significant change in carbon or metal concentrations. The oxygen removal allowed an increase in the density limit by 20%, reduced MARFE-like phenomena, and has lowered Z_{eff} to 1.4 at $\bar{n}_e$ = 4.7 x 10^{19} m^{-3}.

The ohmic heating scaling law,[4] $\tau_E \propto \bar{n}_e q$ established during earlier operational periods, has been confirmed at higher parameter levels: $B_T \leq 4.0$ T and $I_p \leq 2.0$ MA. The density range of TFTR with deuterium plasmas has been extended to $\bar{n}_e$ = 4.7 x 10^{19} m^{-3} because of the density limit $\bar{n}_e^{max} \propto B_T/Rq$ and the application of chromium gettering. The total energy confinement was increased from 0.3 to 0.4 sec at these new operating parameters. Furthermore, there is no clear evidence of saturation of confinement with density. On the other hand, saturation of confinement with density was observed in helium plasmas, where the maximum density achieved was $\bar{n}_e$ = 7.8 x 10^{19} m^{-3} and Z_{eff} = 2 (from neoclassical resistivity) at the high densities. Ion temperatures were not available for this data set, but assuming T_i close to T_i (or the ion thermal conduction is ≈ 3 times the Chang-Hinton ion neoclassical value[15]), the confinement appears to saturate at τ_E ~ 0.35 sec for densities above $\bar{n}_e$ = 5 x 10^{19} m^{-3}.

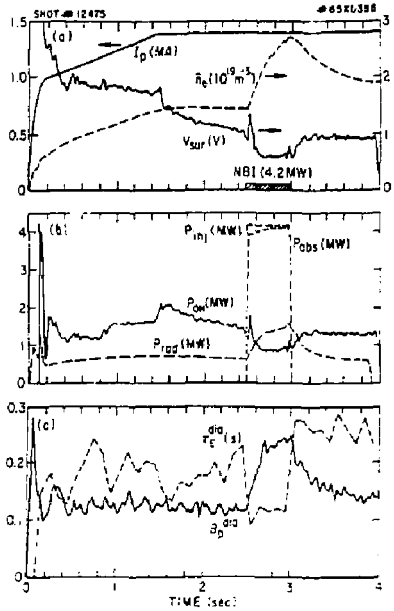

Fig. 1 Evolution of plasma parameters in a beam-heated discharge.

III. CHARACTERISTICS OF BEAM-HEATED DISCHARGES

Figure 1 illustrates the evolution of several plasma parameters for a beam-heated discharge. The discharge is sustained for 4 sec with the flat-top plasma current (I_p) of 1.4 MA (yielding a safety factor q_{cyl} of 3.5 at B_T = 4 T). The total H° beam power of 4.2 MW from two co-tangential beamlines, each with three sources operated at 50-75 keV (62 keV average), is injected for 0.5 sec starting at 2.5 sec. Upon injection the line-averaged electron density ($\bar{n}_e$) is nearly doubled from 1.4 x 10^{19} m^{-3} (without additional gas puff) to 2.7 x 10^{19} m^{-3} primarily due to direct beam fueling, as will be discussed later. The surface voltage (V_{sur}) drops from 1 V to 0.6 V during injection, yielding the ohmic power P_{OH} equal to 1/5 of P_b. The total radiated power (P_{rad}) increases with injection, but the fraction $P_{rad}/(P_{OH} + P_b)$ is reduced to 20%. The value of Z_{eff} of 3.4 (from bremsstrahlung) is in good agreement with the conductivity Z_{eff} of 2.9, particularly considering a calculated beam-driven current of 0.2 MA. Z_{eff} values in beam-heated discharges range between 1.7 and 3.8, and scale as $1/\bar{n}_e$ with only a slight increase of ~ 0.3 from

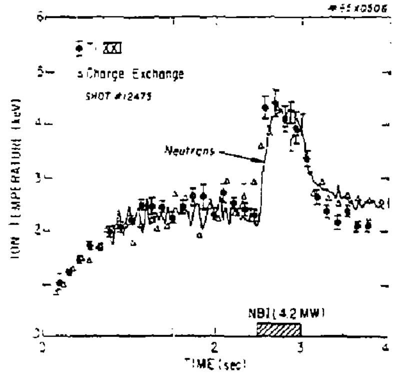

Fig. 2 Evolution of central ion temperature for the discharge shown in Fig. 1.

corresponding OH values. Figure 1(c) shows the evolution of the diamagnetically determined poloidal beta (β_p) and the global energy confinement time derived from it. Values of β_p from the diamagnetic measurement agree reasonably well (within ± 10%) with those calculated by a time-independent snapshot radial profile analysis code (SNAP). Values of $\beta_p + \ell_i/2$ (where ℓ_i is the internal inductivity) from the profile analysis are also in agreement (within ± 10%) with those from the magnetic equilibrium measurement.

Figure 2 shows the time behavior of the central ion temperature [$T_i(o)$] for the discharges shown in Fig. 1 as derived from three different diagnostics: Doppler broadening of Ti XXI Kα line radiation, charge exchange analysis, and total neutron emission. The $T_i(o)$ values increase from 2 keV to 4.4 keV upon injection. Under these operating conditions, corrections to the $T_i(o)$ values in the Ti XXI Kα and charge exchange measurements are small and their agreements are satisfactory. However, the neutron emission measurement requires an assumption that the density rise during injection is solely due to injected protons rather than due to recycling deuterons, as well as knowledge of the deuteron density before injection. Electron temperature profiles are measured by Thomson scattering, fundamental (heterodyne radiometer) and second harmonic (Michelson interferometer) electron cyclotron emission diagnostics. Electron heating has been small under usual operating conditions. There are two contributing factors. The first is the strong rise in electron density which masks the temperature increase. However, when a T_e profile with injection is compared with a T_e profile with OH alone at the same density, a notable increase in T_e is seen across the discharge. The other contributing factor is

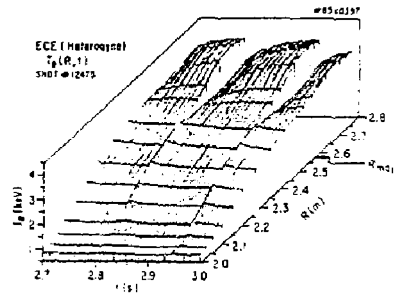

Fig. 3 Giant sawtooth oscillations in electron temperature profile during injection.

large sawtooth oscillations frequently accompanying the injection. Figure 3 depicts giant sawteeth in $T_e(r)$ measured by the ECE (heterodyne radiometer) diagnostic in the discharge shown in Fig. 1.

IV. NEUTRAL BEAM POWER DEPOSITION

We have seen in Fig. 1(c) that the global energy confinement, τ_E^{dia} decreases during injection and recovers quickly after injection, indicating that the increase in β_p (or the stored energy) with injection is not large enough. This point is also illustrated in Fig. 4 where the total stored energy, the sum of the electron (W_e) and ion (W_i) stored energy determined from the profile analysis, is plotted as a function of the total heating power ($P_{OH} + P_{abs}$). Compared with the stored energy gained by OH discharges in a similar density range, the increase in the total stored energy with additional neutral beam power is relatively small. This suggests that we should be concerned about the possibility that the beam power injected and deposited into the plasma is less than estimated. However, the following four observations eliminate this possibility. (1) Substantial efforts in the NB operation part were made to improve the accuracy of the beam power measurements.[7] Based on the measurements, the calibration factor for H° injection has been lowered relative to the previous power estimates by 15%.[6] (2) Nearly 100% power accountability at plasma boundaries has been demonstrated with two methods. The first method involves a deliberate enhancement of radiative loss with neon injection. As shown by the upper right point in Fig. 5, addition of neon (~ 3% of the total electrons) has produced radiative loss of up to 100% of the total input power with a negligible power to the limiter. The second method for the power accountability involves simultaneous measurements of losses to the walls and to the limiter. The loss to the wall is measured by

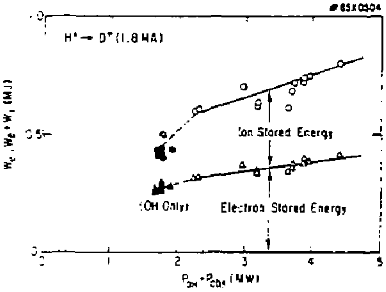

Fig. 4 Plasma stored energies as function of the total input power.

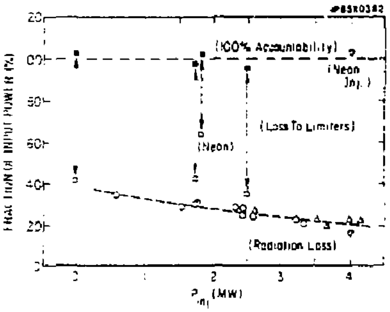

Fig. 5 Power accountability from measurements of radiation loss and power to the limiter with and without neon injection.

bolometer arrays, and the loss to the limiter is determined by infrared television in conjunction with a heat-transfer model.[16] Figure 5 shows an excellent power accountability (100 ± 10%) in most cases. We note that the shinethrough of the tangential beams is calculated to be small (< 5%). Furthermore, the successful accountability implies that the fast ion charge exchange loss (preferentially in the forward direction beyond the acceptance angles of the bolometer arrays) is small, as indicated by Monte-Carlo calculations.[17] (3) The particle accountability of beam injection also supports the conclusion that the neutral beam power is delivered as expected. Figure 6 shows that the increment of the line-averaged electron density observed at the end of a 0.5 sec beam pulse agrees well with that calculated from the number of beam particles and the global particle confinement time (τ_p^*) for H° injection. The values of τ_p^* plotted in Fig. 6

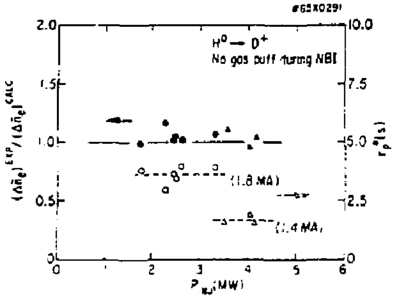

Fig. 6 Ratio of the observed to calculated density rise during injection and the global particle confinement time versus injection power.

are calculated at 0.2 sec after the beam turn-off, although τ_p^* values during injection are not much different from those after injection (i.e., there is no substantial "density clamping"[18] at these high I_p). At low I_p (0.8 MA) with D° injection, τ_p^* during injection is decreased to 0.2–0.4 sec, and the small τ_p^* made it possible to attain the energetic-ion regime at low $\bar{n}_e$.[9] (4) Poor beam penetration resulting from injection of low-energy beams into the large size plasmas can in principle lead to the poor heating performance. Monte-Carlo calculations of power deposition[19] show substantial differences between H° and D° injection under similar experimental conditions, as shown in Fig. 7. On the other hand, the plasma performance of the poorly penetrating D° beams proves to be as good as or even better than that of H° beams, as indicated by $T_i(0)$ or gross energy confinement times tabulated in Table 1. Based on these observations, we conclude that the beam power is delivered to the plasma and that the less-than-expected increase in plasma energy content represents a deterioration of energy confinement.

V. SCALING OF ENERGY CONFINEMENT TIMES

The dependence of the energy confinement time on plasma density, beam power, and plasma current has been examined with H° and D° beam powers up to 5 MW into the large plasmas (R_0 = 2.58 m, a = 0.81 m) at B_T = 4.0 T. In these experiments, the plasma current has been varied from 0.8 MA to 1.8 MA, and scans of density and beam power have been taken at each step. Figure 8 shows gross energy confinement times [$\tau_E(a)$] as functions of $\bar{n}_e$ with and without NBI, where $\tau_E(a) = (W_e + W_i)/(P_{OH} - P_{oe} + P_{bi})$ evaluated at r = a using the profile analysis. In contrast to the OH confinement which follows closely the TFTR scaling, $\tau_E(a)$ with injection is independent of $\bar{n}_e$. The figure also shows that values of

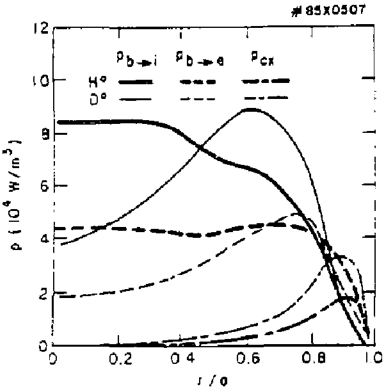

Fig. 7 Comparison of power deposition profiles for H° and D° injection. Plasma parameters are listed in Table 1.

Table 1

Comparison Between H° and D° Injection

(I_p = 1.8 MA, B_T = 4.0 T,

$\bar{n}_e$ = 4.4 x 10^{19} m^{-3}, P_b = 3.3 MW)

Beam	$\tau_E(o)$ (s)	$\tau_E(a/2)$ (s)	$\tau_E(a)$ (s)	$T_i(o)$ (keV)	$T_e(o)$ (keV)
H°	0.20	0.24	0.19	2.8	2.6
D°	0.26	0.28	0.20	2.6	2.4

$\tau_E(a)$ are in accord with those predicted by the Goldston L-mode scaling[19] which was established with data from beam-heated discharges with degrading confinement in smaller devices. Figure 9 illustrates similar constancy of the global energy confinement time $[\tau_E^{dia} = (W_e + W_i + 3W_{bi}/2)/(P_{OH} + P_{abs})]$ with $\bar{n}_e$ for different I_p and injected beam species. There exists some difference in the definitions of τ_E^{dia} from $\tau_E(a)$. However, small fast ion energy (W_{bi}) and fast ion charge exchange loss (= $P_{abs} - P_{be} - P_{bi}$) tend to compensate each other, making τ_E^{dia} nearly equal to $\tau_E(a)$ under normal experimental conditions. However, τ_E^{dia} at low $\bar{n}_e$ with I_p = 0.8 MA includes substantial beam contributions and charge exchange loss[9] as well as plasma rotation energy.

Figure 10 illustrates the dependence of $\tau_E(a)$ on beam power, indicating that confinement degrades at high beam power. Figure 11 plots $\tau_E(a)$ as a function of I_p,

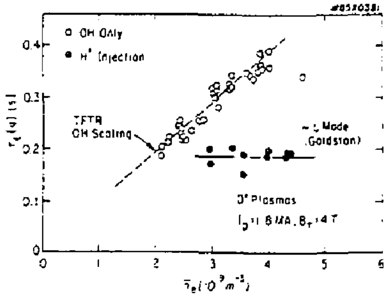

Fig. 9 Density dependence of gross energy confinement time (determined from the profile analysis) with and without injection.

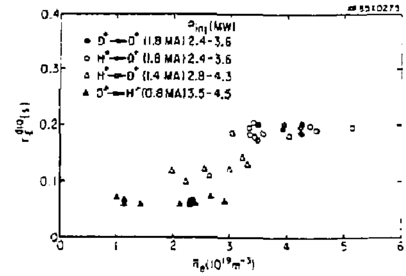

Fig. 9 Density dependence of global energy confinement time (derived from the diamagnetic measurement).

showing that $\tau_E(a)$ increases roughly linearly with I_p. The best fit of these data shown in Fig. 8 and 9 is expressed as $\tau_E = I_p^{.3} (P_{OH} + P_{abs})^{-0.57}$. This fit has very similar parametric dependencies as either the Goldston[19] or Kaye-Goldston[20] L-mode scalings. Within the scatter of the data, it can be fit also to a form of a + b/(P_{OH} + P_{abs}), as previously suggested. The strong dependence of τ_E on I_p is encouraging. Indeed, τ_E values of 0.2 sec have been obtained at I_p = 1.8 MA with injection power substantially higher (by factor > 2) than P_{OH}.

VI. DISCUSSIONS AND CONCLUSIONS

In an attempt to understand the mechanisms responsible for the confinement deterioration, transport studies are being carried out primarily with two transport codes: the time-independent SNAP code for wide survey of transport parameters; and the time-dependent TRANSP code[21] for detailed studies of transport characteristics in selected discharges. Thus far the TRANSP runs have concentrated on two typical NBI discharges.

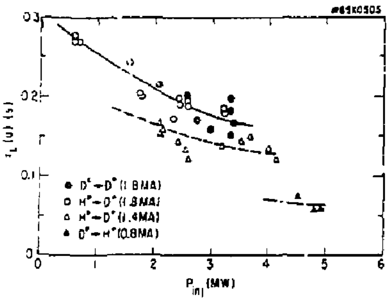

Fig. 10 Beam power dependence of gross energy confinement time.

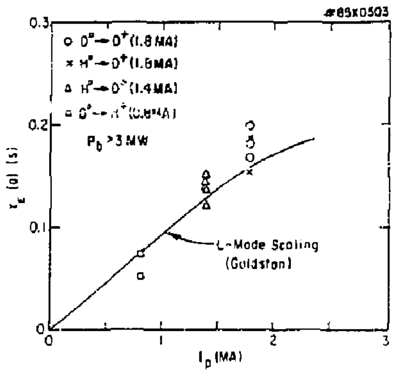

Fig. 11 Plasma current dependence of gross energy confinement, and comparison with the Goldston L-mode scaling.

(1) In a high density case [H°(3.2 MW) + D^+ (1.8 MA), $\bar{n}_e$ = 4.3 x 10^{19} m^{-3}], $T_i(o)$ tracks closely with $T_e(o)$ due to strong electron-ion coupling, as in the usual injection cases. Although the difference between $T_e(o)$ and $T_i(o)$ is not known well enough to determine precisely the multiplier on the Chang-Hinton ion neoclassical conductivity,[15] a multiplier of 3 is adequate to reproduce the experimental $T_i(o)$ and total stored energy. Then the power balance indicates that $\tau_{Ei}(2a/3)$ exceeds $\tau_{Ee}(2a/3)$ by a factor of 5. Therefore it seems reasonable to conclude that the electron loss channel is responsible for the confinement deterioration in higher density discharges. (2) In a low-density, high-power case [H°(4.2 MW) + D^+(1.4 MA), $\bar{n}_e$ = 2.6 x 10^{19} m^{-3}, as shown in Figs. 1-3], the ion-electron coupling becomes weak relative to beam power input to ions. There τ_{Ei} becomes comparable to τ_{Ee} at least at $r < 2a/3$, indicating that the ion loss channel becomes significant in the overall confinement. Although a somewhat larger multiplier appears necessary to match the experimental $T_i(o)$ shown in Fig. 2, its precise determination requires knowledge of the convective loss which may become important in this high ion temperature plasma.

Clearly further analyses are required to understand transport characteristics in these discharges. At the same time, several new effects must be incorporated in the transport analysis. The giant sawtooth oscillation (as in Fig. 3) may be important in thermal energy confinement in the core plasma as well as in fast ion confinement. The maximum toroidal rotation velocity observed in TFTR has been 6 x 10^5 m/sec in the low-$\bar{n}_e$, 0.8 MA discharges, although velocities of 2 x 10^5 m/sec are typical in the normal operating regime. These velocities become a significant fraction of the thermal ion velocity (up to 0.8), and should be taken into account in the transport analyses. MHD activity, fluctuations, and plasma edge conditions may have to be considered.

The main objective of this run period has been to extend the plasma performance with the improved device capabilities, and significant progress has been made in this regard. τ_E of 0.4 sec has been obtained in a clean (Z_{eff} = 1.4) OH discharge. With injection of beam power up to 5 MW, we have achieved the highest *ion temperature* of 5 keV under normal operating conditions, and even higher $T_i(o)$ in the energetic-ion regime.[9] Despite the confinement deterioration (or the L-mode scaling), high-current operation is clearly advantageous and has achieved τ_E of 0.2 sec with neutral power significantly higher than ohmic power. We look forward to further upgrades of I_p and B_T to the maximum design capabilities in the near future.

The other major objective of the present run period has been to improve the plasma performance using novel discharge scenarios. Among various schemes attempted so far has been the neon injection into beam-heated discharges (Z-mode).[22] Although some encouraging results have been observed and cooling of the limiters with neon injection has been clearly demonstrated, a substantial increase in τ_E at higher $\bar{n}_e$ is yet to be seen. Shifting the plasma column to the inner wall is of special interest from the viewpoint of the future program[16] and possible confinement improvement. The most important confinement improvement scheme yet to be tried is pellet injection. A pneumatic multiple pellet injector[23] has been installed on TFTR and the experiment is now starting.

ACKNOWLEDGMENTS

It is a real pleasure to acknowledge the very many engineers, computer programmers, and technicians whose dedicated efforts have enabled us to conduct these experiments. Special thanks are due to J. Strachan for discussions. The work was supported by US Department of Energy Contract No. DE-AC02-76-CHO3073. The ORNL participants were also supported by US Department of Energy Contract No. DE-AC05-84OR 21400 with Martin Marietta Energy Systems, Inc.

REFERENCES

1. K. M. YOUNG et al., Plasma Phys. 26, 11 (1984).

2. P. C. EFTHIMION et al., Phys. Rev Lett. 52, 1492 (1984).

3. R. J. HAWRYLUK et al., Proc 4th Intl. Symp. on Heating in Toroidal Plasmas, Rome (Intl. School of Plasma Physics, Varenna, 1984) p. 1012.

4. P. C. EFTHIMION et al., Plasma Physics and Controlled Nuclear Fusion Research (Proc. 10th Int. Conf., London, 1984) IAEA, Vienna (1985), IAEA-CN-44/A-I-2.

5. G. D. TAIT et al., ibid, IAEA-CN-44/A-III-1.

6. H. P. EUBANK et al., ibid, IAEA-CN-44/A-V-3.

7. M. D. WILLIAMS et al., "Neutral Beam Heating System for TFTR," Session B, present meeting.

8. J. MCCANN and M. VIOLA, "Operations Analysis of the Unscheduled Summer Machine Opening on TFTR," Session 2D-2, present meeting.

9. H. P. FURTH, "The TFTR Experimental Research Program," invited paper, Session 1A, present meeting.

10. M. G. BELL et al., "Plasma Operating Modes and Control in TFTR," Session 3D-4, present meeting.

11. K. W. HILL, et all, "Studies of Impurity Behavior in TFTR," Session 6D-2, present meeting.

12. B. LIPSCHULTS et al., Nucl. Fusion 24, 977 (1984).

13. J. COONROD and J. SCHIVELL, "Plasma Disruption Characteristics in TFTR," Session 3D-4, present meeting.

14. P. K. MIODUSZEWSKI et al., "Chromium Gettering in ISX-B," to be published in J. Nucl. Mater.

15. C. S. CHANG and F. L. HINTON, Phys. Fluids 25, 1493 (1982).

16. M. ULRICKSON et al., "The Interaction of Physics and Engineering in the Design of TFTR First Wall Components," Session 3D-4, present meeting.

17. R. J. GOLDSTON et al., J. Comput. Phys. 43, 61 (1981).

18. D. W. SWAIN et al., Controlled Fusion and Plasma Physics (Proc. 9th European Conference, Oxford, 1979) Culham Laboratory 44 (1979).

19. R. J. GOLDSTON, Plasma Physics and Controlled Fusion 26, 87 (1984).

20. S. M. KAYE and R. J. GOLDSTON, Nucl. Fusion 25, 65 (1985).

21. R. J. HAWRYLUK et al., Proc. of the Course in Physics Close to Thermonuclear Conditions (Varenna, Italy), Report EUR-FU-BRU/XII/475/80.

22. E. A. LAZARUS et al., J. Nucl. Mater. 121, 61 (1984).

23. S. L. MILORA et al., "Pellet Fueling: State of the Art Development and Applications," Session 4B, present meeting.

EXTERNAL DISTRIBUTION IN ADDITION TO UC-20

Plasma Res Lab, Austra Nat'l Univ, AUSTRALIA
Dr. Frank J. Paoloni, Univ of Wollongong, AUSTRALIA
Prof. I.R. Jones, Flinders Univ., AUSTRALIA
Prof. M.H. Brennan, Univ Sydney, AUSTRALIA
Prof. F. Cap, Inst Theo Phys, AUSTRIA
Prof. Frank Verheest, Inst theoretische, BELGIUM
Dr. D. Palumbo, Dg XII Fusion Prog, BELGIUM
Ecole Royale Militaire, Lab de Phys Plasmas, BELGIUM
Dr. P.H. Sakanaka, Univ Estadual, BRAZIL
Dr. C.R. James, Univ of Alberta, CANADA
Prof. J. Teichmann, Univ of Montreal, CANADA
Dr. H.M. Skarsgard, Univ of Saskatchewan, CANADA
Prof. S.R. Sreenivasan, University of Calgary, CANADA
Prof. Tudor W. Johnston, INRS-Energie, CANADA
Dr. Hannes Barnard, Univ British Columbia, CANADA
Dr. M.P. Bachynski, MPB Technologies, Inc., CANADA
Chalk River, Nucl Lab, CANADA
Zhengwu Li, SW Inst Physics, CHINA
Library, Tsing Hua University, CHINA
Librarian, Institute of Physics, CHINA
Inst Plasma Phys, Academia Sinica, CHINA
Dr. Peter Lukac, Komenskeho Univ, CZECHOSLOVAKIA
The Librarian, Culham Laboratory, ENGLAND
Prof. Schatzman, Observatoire de Nice, FRANCE
J. Radet, CEN-BP6, FRANCE
AM Dupas Library, AM Dupas Library, FRANCE
Dr. Tom Mual, Academy Bibliographic, HONG KONG
Preprint Library, Cent Res Inst Phys, HUNGARY
Dr. S.K. Trehan, Panjab University, INDIA
Dr. Indra Mohan Lal Das, Banaras Hindu Univ, INDIA
Dr. L.K. Chavda, South Gujarat Univ, INDIA
Dr. R.K. Chhajlani, Vikram Univ. INDIA
Dr. B. Dasgupta, Saha Inst, INDIA
Dr. P. Kaw, Physical Research Lab, INDIA
Dr. Phillip Rosenau, Israel Inst Tech, ISRAEL
Prof. S. Cuperman, Tel Aviv University, ISRAEL
Prof. G. Rostagni, Univ Di Padova, ITALY
Librarian, Int'l Ctr Theo Phys, ITALY
Miss Clelia De Palo, Assoc EURATOM-ENEA, ITALY
Biblioteca, del CNR EURATOM, ITALY
Dr. H. Yamato, Toshiba Res & Dev, JAPAN
Direc. Dept. Lg. Tokamak Dev. JAERI, JAPAN
Prof. Nobuyuki Inoue, University of Tokyo, JAPAN
Research Info Center, Nagoya University, JAPAN
Prof. Kyoji Nishikawa, Univ of Hiroshima, JAPAN
Prof. Sigeru Mori, JAERI, JAPAN
Library, Kyoto University, JAPAN
Prof. Ichiro Kawakami, Nihon Univ, JAPAN
Prof. Satoshi Itoh, Kyushu University, JAPAN
Dr. D.I. Choi, Adv. Inst Sci & Tech, KOREA
Tech Info Division, KAERI, KOREA
Bibliotheek, Fom-Inst Voor Plasma, NETHERLANDS
Prof. B.S. Liley, University of Waikato, NEW ZEALAND
Prof. J.A.C. Cabral, Inst Superior Tech, PORTUGAL
Dr. Octavian Petrus, ALI CUZA University, ROMANIA
Prof. M.A. Hellberg, University of Natal, SO AFRICA
Dr. Johan de Villiers, Plasma Physics, Nucor, SO AFRICA
Fusion Div. Library, JEN, SPAIN
Prof. Hans Wilhelmson, Chalmers Univ Tech, SWEDEN
Dr. Lennart Stenflo, University of UMEA, SWEDEN
Library, Royal Inst Tech, SWEDEN
Centre de Recherchesen, Ecole Polytech Fed, SWITZERLAND
Dr. V.T. Tolok, Kharkov Phys Tech Ins, USSR
Dr. D.D. Ryutov, Siberian Acad Sci, USSR
Dr. G.A. Eliseev, Kurchatov Institute, USSR
Dr. V.A. Glukhikh, Inst Electro-Physical, USSR
Institute Gen. Physics, USSR
Prof. T.J.M. Boyd, Univ College N Wales, WALES
Dr. K. Schindler, Ruhr Universitat, W. GERMANY
Nuclear Res Estab, Julich Ltd, W. GERMANY
Librarian, Max-Planck Institut, W. GERMANY
Bibliothek, Inst Plasmaforschung, W. GERMANY
Prof. R.K. Janev, Inst Phys, YUGOSLAVIA